Tests of Chiral Perturbation Theory with COMPASS

Jan Friedrich

Physik-Department, Technische Universität München, Germany

for the COMPASS collaboration

Abstract. The COMPASS experiment at the CERN SPS studies with high precision pion-photon induced reactions via the Primakoff effect on nuclear targets. This offers the test of chiral perturbation theory (ChPT) in various channels: Pion Compton scattering allows to clarify the long-standing question of the pion polarisabilities, single neutral pion production is related to the chiral anomaly, and for the two-pion production cross sections exist as yet untested ChPT predictions.

Keywords: chiral perturbation theory, pion and kaon polarisabilities, chiral anomaly, COMPASS
PACS: 12.39.Fe, 13.40.Em, 13.60.Fz, 13.75.Lb, 14.40.Be

Introduction

COMPASS [1] investigates hadron structure and spectroscopy by various methods, scattering hadron and muon beams with up to 200 GeV/c from the CERN SPS facility off fixed targets. Connecting high rate capability with high precision, it is ideally suited to study pion-photon induced reactions via the Primakoff effect on nuclear targets.

In [2] the Weizsäcker-Williams method has been generalized to any reaction of an incoming charged particle colliding with a photon of the nuclear Coulomb field. The cross section decomposes into a virtual (quasi-real) photon density and the real-photon cross section,

$$\frac{d\sigma}{ds\,dt_r\,dt} = \frac{\alpha}{\pi(s-m_\pi^2)} \cdot F^2_{\mathrm{eff}}(t) \cdot \frac{t'}{t^2} \cdot \frac{d\sigma_{\pi\gamma}(s)}{dt_r} \tag{1}$$

where $t' = |t| - |t|_{\mathrm{min}}$ is the momentum transfer to the nucleus, $|t|_{\mathrm{min}} = [(s-m_\pi^2)/2E_{\mathrm{beam}}]^2$, and s and t_r are the Mandelstam variables in the real-photon subprocess.

The real-photon processes discussed in the following are

$$\pi^- + \gamma \rightarrow \begin{cases} \pi^- + \gamma & \text{Compton reaction} \\ \pi^- + \pi^0 & \text{chiral anomaly} \\ \pi^- + \pi^- + \pi^+ & \text{two-pion production} \end{cases} \tag{2}$$

In Fig. 1, the full photon-exchange process is shown, examplary for two-pion production, together with the competing production of the same final state through strong interaction, govered by pomeron exchange at high beam energy.

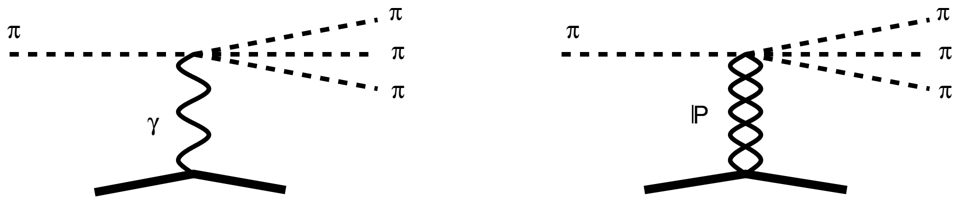

FIGURE 1. Reaction mechanisms in pion-nucleus scattering at low momentum transfer, examplary for the two-pion production reaction $\pi N \to N\pi\pi\pi$. On the left graph, the pion scatters off a quasi-real photon of the nuclear Coulomb field, which dominates at extremely small momentum transfers q^2. At higher q^2, the strong interaction with the nucleus leads to diffractive dissociation of the incoming pion, described by the exchange of a soft pomeron.

Compton scattering

Measuring Compton scattering via the Primakoff effect allows to clarify the long-standing question of the pion polarisabilities with unprecedented precision. In the real-photon process, electric and magnetic dipole polarisabilities α_π, β_π and the quadrupole polarisabilities α_2, β_2 enter via

$$\begin{aligned}\frac{\mathrm{d}\sigma_{\pi\gamma}}{\mathrm{d}\Omega_{cm}} &= \frac{\alpha^2(s^2z_+^2+m_\pi^4z_-^2)}{s(sz_+ + m_\pi^2 z_-)^2} - \frac{\alpha\, m_\pi^3\,(s-m_\pi^2)^2}{4s^2(sz_+ + m_\pi^2 z_-)} \cdot \\ &\cdot \left[z_-^2\,(\alpha_\pi - \beta_\pi) + \frac{s^2}{m_\pi^4} z_+^2\,(\alpha_\pi + \beta_\pi) - \frac{(s-m_\pi^2)^2}{24s} z_-^3\,(\alpha_2 - \beta_2)\right] \qquad (3)\end{aligned}$$

where $z_\pm = 1 \pm \cos\theta_{cm}$, θ_{cm} the scattering angle in the CM system of the outgoing $\pi\gamma$ pair. The effect expected from the polarisability values of ChPT in 2-loop order [3] is depicted in Fig. 2. It deviates by about a factor 2 from some earlier measurements, including the only preceding Primakoff measurement at Serpukhov [4], while the overall experimental situation is inconsistent [5].

COMPASS has shown in a short pilot run 2004 that the apparatus is capable of measuring and identifying the wanted process, collecting within a few days a statistics exceeding that of the Serpukhov experiment. Due to the preliminary character of the setup, the trigger involved a complicated inefficiency that was not correctable in the analysis on a sufficiently accurate level in order to extract the pion polarisabilities. With a new approach for the trigger on the electromagnetic calorimeter, processing the signals by a digital module, a new set of data with the same order of statistics as 2004 has recently been taken (Nov. 2009). A first look into these data is promising, while the final analysis will still take some time.

In order to address all the unknown quantities contained in Eq. 3, i.e. an independent extraction of the dipole polarisabilities and a determination of the quadrupole term, a much higher statistics must be taken. A proposal for such a Primakoff beam time has been made for COMPASS-II [6], increasing the existing statistics by at least a factor 30. Along with this measurement, identifying the kaon component of the incoming beam by CEDAR detectors will allow to also extract the kaon polarisabilities for the first time.

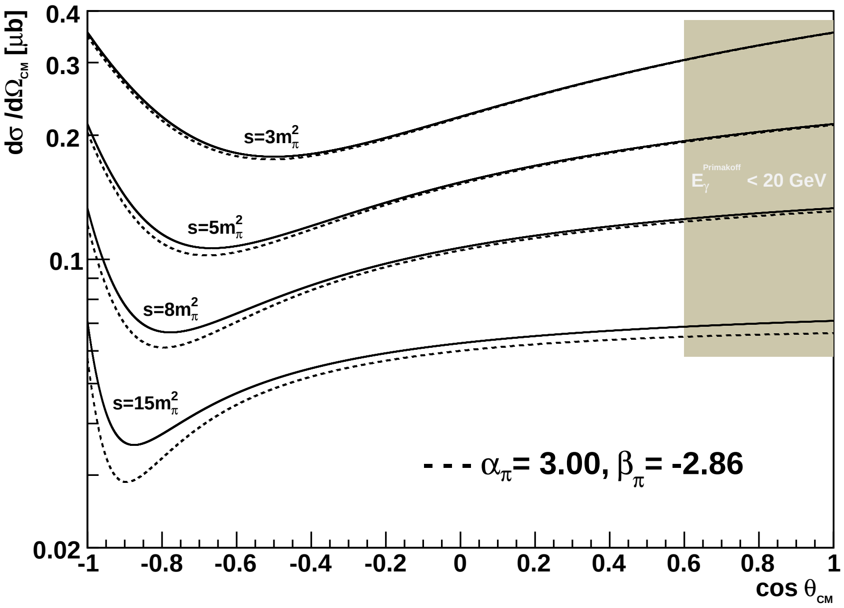

FIGURE 2. Effect of the pion polarisability on the cross section of pion Compton scattering $\pi\gamma \to \pi\gamma$. The pure Born graph calculation for a pointlike pion is shown as continuous lines, while the effect of the polarisabilities is is included in the dashed curves ($\alpha_\pi = 3 \cdot 10^{-4}\mathrm{fm}^3$, $\beta_\pi = -2.86 \cdot 10^{-4}\mathrm{fm}^3$). The effect increases with larger CM energy, at forward angles also the small non-zero value of $\alpha_\pi + \beta_\pi$ causes a measurable deviation. Loop contributions are not included. The shaded region corresponds to low photon energy $E_\gamma < 20$ GeV in the laboratory, which is not covered in the data taking.

Chiral anomaly

Since the measurement of the Compton reaction is triggered by the photon signal in the electromagnetic calorimeter, also the production of neutral pions is detected, observing the two decay photons from $\pi^0 \to \gamma\gamma$. On the one hand, this is important because the decay photons partially contribute to the background for the Compton reaction, in case the separation of the two photon clusters in the calorimeter does not succeed, or in case the softer decay photon remains undetected. This can be controlled by determining the strength of π^0 production from two detected photons and extrapolating to the concerned kinematical regions.

On the other hand, single neutral pion production is interesting by itself, as its strengh challenges the existing prediction for the chiral anomaly constant $F_{3\pi}$. While there exists a single experimental result obtained from the Serpukhov data, which is in fair agreement with this prediction, new COMPASS data can contribute to a much more precise test.

The 2004 COMPASS data on the $\pi^-\pi^0$ final state have been affected by the same trigger inefficiency as described for the Compton reaction, leading to a similar conclusion concerning a precise determination of $F_{3\pi}$ as the polarisabilities. Some plots of the analysis of the 2004 data are presented in [6].

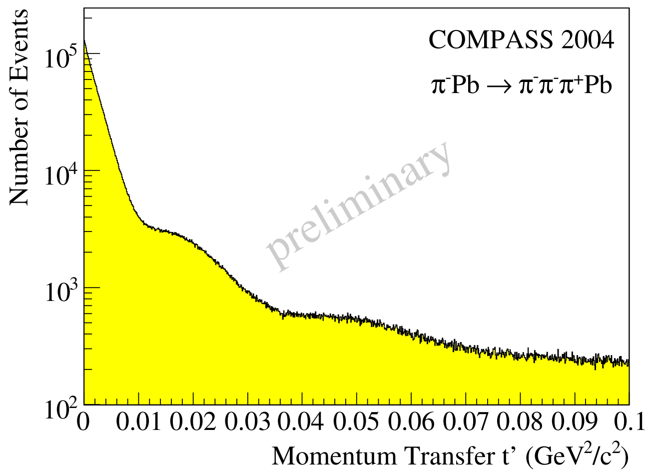

FIGURE 3. Measured momentum transfer spectrum in the reaction $\pi^- \mathrm{Pb} \to \mathrm{Pb}\pi^-\pi^-\pi^+$. The Primakoff region $t' < 0.001$ GeV$^2/c^2$ covers only the lowest bins of the distribution, the adjacent low-t' region up to $t' < 0.01$ GeV$^2/c^2$ shows the characteristic $e^{-bt'}$ behaviour of a diffractive process.

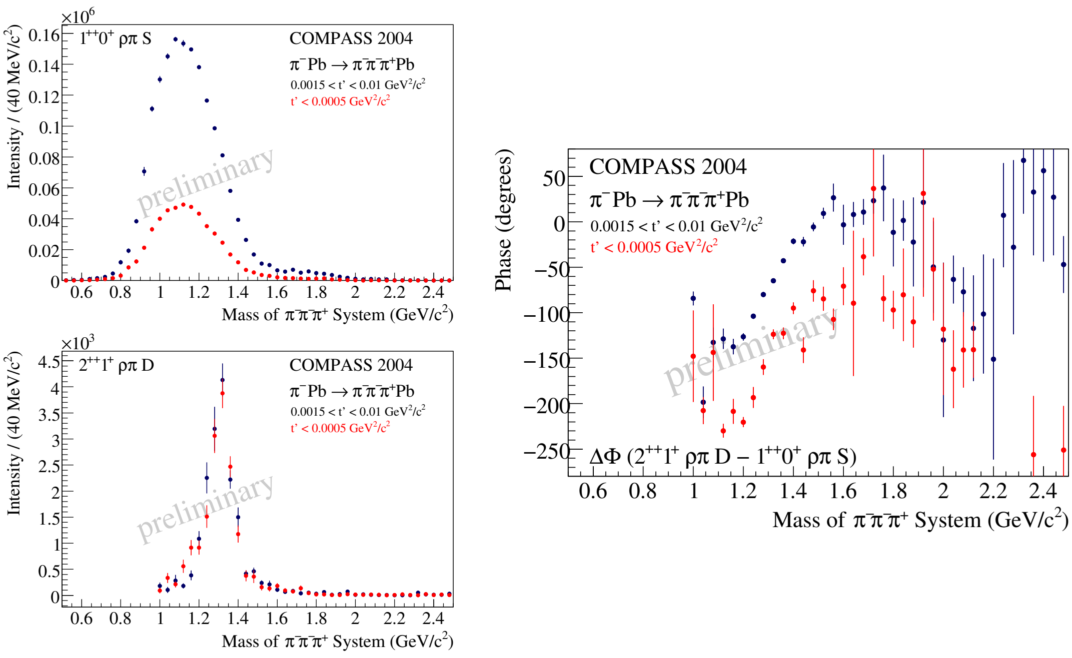

FIGURE 4. Result of the partial wave analysis for the $1^{++}0^+$ and $2^{++}1^+$ contributions in different t' windows. The intensity of the a_2 signal is about equal in the Primakoff $t' < 0.0005$ and in the low-t' range $0.0015 < t' < 0.01$, while the a_1 Primakoff signal is about a factor 3 weaker. In both cases, the phase between the the two waves exhibits the walk of the narrow a_2 resonance on the high-energetic tail of the a_1 (right graph). Their position is relatively shifted by about 90°, indicating the different production phases introduced by the exchange of a photon or a pomeron, respectively.

Two-pion production

In addition to the electromagnetic trigger, a trigger on the multiplicity of charged particles downstream the lead target was implemented in the 2004 setup. As it is not affected by the trigger inefficiency of the neutral channels, the analysis could be pursued to a high level of precision. For the region of high momentum transfer $|t| > 0.1$ GeV^2/c^2 in $\pi^-\mathrm{Pb} \rightarrow \mathrm{Pb}\pi^-\pi^-\pi^+$, a partial wave analysis has been performed, leading to the observation of a $J^{PC} = 1^{-+}$ exotic state [9]. The spectrum of low momentum transfer of the same final state is presented in Fig. 3. The partial wave analysis has been performed in two steps, owing to the different production mechanisms involved: First, the t' spectrum was examined in two windows, one for the Primakoff region $t' < 0.0005$ GeV^2/c^2 and one for the low-t' region, 0.001 GeV^2/c$^2 < t' < 0.01$ GeV^2/c^2. In both windows the main resonances $a_1(1260)$ and $a_2(1320)$ are observed with their respective quantum numbers, the a_1 strength being relatively suppressed in the Primakoff region compared to the diffractive low-t' region, cf. Fig. 4. The phase motion is similar in both cases, but its position is shifted between the two cases, pointing to the different production mechanisms.

Secondly, the analysis was performed in finer t' slices, presented in Fig. 5. Here, the strength of the a_2 at very low t' shows the steep rise characteristic for Primakoff production, convoluted with the experimental resolution. This very clear signal triggered a closer look at the full mass spectrum of the 3-pion final state in Primakoff production. By statistical subtraction, using the exponential fall of the t' distribution as diffractive background estimate, the 3-pion mass spectrum in Fig. 6 has been obtained. Exceeding the precision of the SELEX statistics [8], it appears feasable to extract for the first time the strength of the $\pi\gamma \rightarrow 3\pi$ reaction close to its threshold, for which a, yet untested, tree graph calculation from ChPT [5] exists.

Acknowledgments

This work is supported by the Federal Ministry of Education and Research (BMBF), the Maier-Leibnitz-Labor München, the DFG cluster of excellence EXC153 and CERN-RFBR 08-02-91009.

REFERENCES

1. COMPASS collaboration (P. Abbon *et al.*), Nucl. Instr. Meth. **A577**, 455 (2007).
2. I. Y. Pomeranchuk, I. M. Shmushkevich, Nucl. Phys. **23** (1961) 452.
3. U. Bürgi, Nucl. Phys. **B479**, 392 (1996), Phys. Lett. **B377** (1996).
4. Y. Antipov *et al.*, Phys. Lett. **B121**, 445 (1983).
5. N. Kaiser, J. M. Friedrich, Eur. Phys. J. **A36**, 181 (2008).
6. COMPASS-II Proposal, `http://wwwcompass.cern.ch/compass/proposal/compass-II_proposal/compass-II_proposal.pdf`
7. G. Fäldt, U. Tengblad, Phys. Rev. **C79**, 014607 (2009).
8. SELEX collaboration (V. V. Molachanov *et al.*), Phys. Lett. **B521**, 171 (2001).
9. COMPASS collaboration (M. G. Alekseev *et al.*), Phys. Rev. Lett. **104**, 241803 (2010).

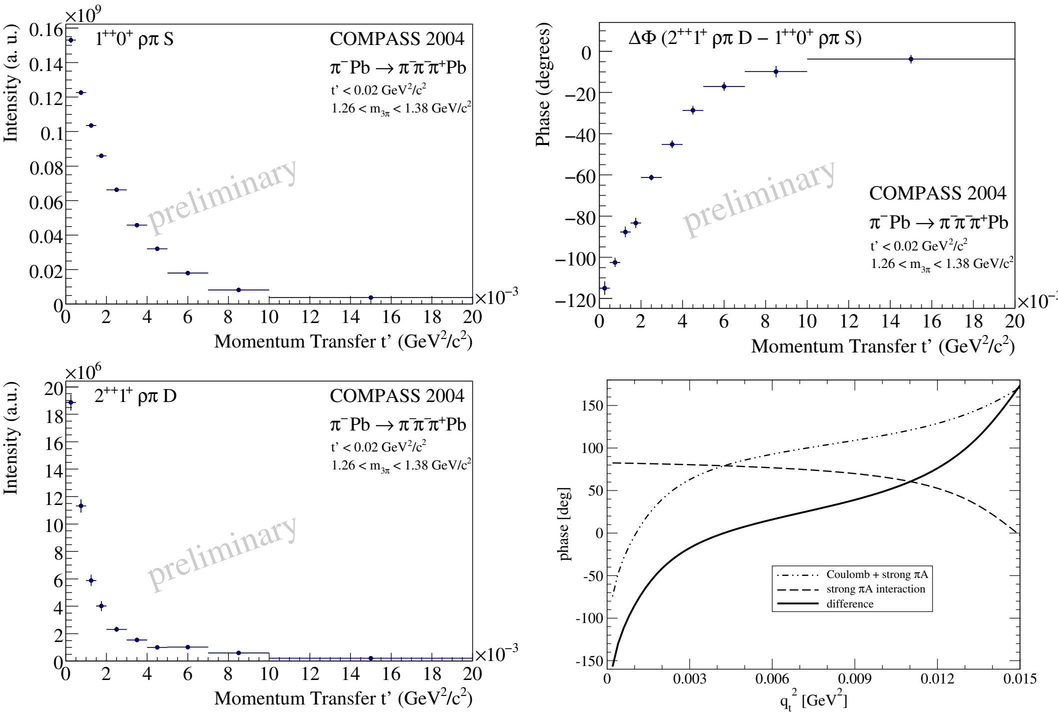

FIGURE 5. Result of the partial wave analysis for the two waves as in Fig. 4, now in fine t' slices. Plots on the left: While the intensity of the a_1 follows about the t' dependence of the diffractive slope (cf. Fig. 3), the a_2 signal features the steep Primakoff rise at small t'. The relative phase difference (upper right plot) vanishes with increasing t', indicating that at higher momentum transfer the production mechanism for a_2 becomes dominated by strong interacting, as it is for the a_1. The lower-right plot shows this phase walk evaluated in the Glauber model following [7].

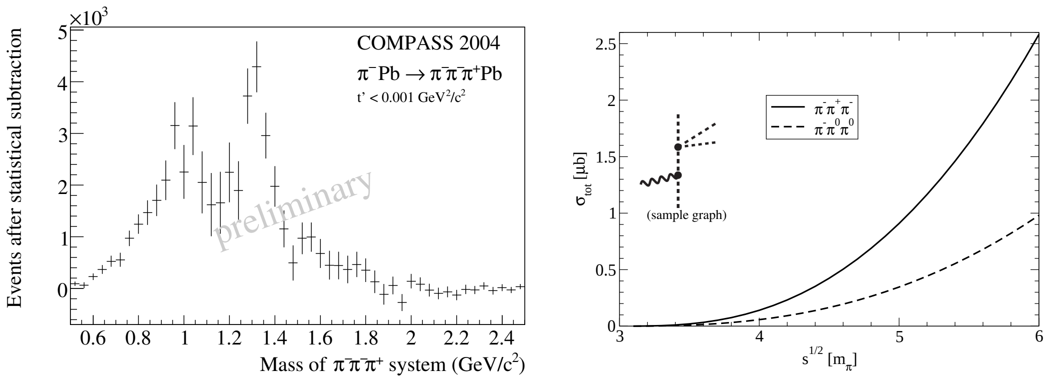

FIGURE 6. Left: Measured Primakoff 3π mass spectrum obtained by statistical subtraction, analogously to the SELEX analysis [8]. Apart from the a_2 signal, it features a broader distribution peaking around 1 GeV. Its low-energetic tail is to be compared to the ChPT prediction (right plot, from [5]), once the experimental distribution is properly normalized.